CHEMISTRY
AN ASIAN JOURNAL
www.chemasianj.org

Accepted Article

Title: Cu(II) and Na(I) complexes based on 3,7-Diacetyl-1,3,7-triaza-5-phosphabicyclo[3.3.1]nonane-5-Oxide (DAPTA=O): synthesis, characterization and catalytic activity

Authors: Maria de Fátima C. Guedes da Silva, Abdallah G. Mahmoud, Ewelina I. Śliwa, Piotr Smoleński, Maxim L. Kuznetsov, and Armando J. L. Pombeiro

To be cited as: *Chem. Asian J.* 10.1002/asia.201800799

Link to VoR: http://dx.doi.org/10.1002/asia.201800799

A Journal of
ACES Asian Chemical Editorial Society

A sister journal of Angewandte Chemie and Chemistry – A European Journal

WILEY-VCH

10.1002/asia.201800799

Cu(II) and Na(I) complexes based on 3,7-Diacetyl-1,3,7-triaza-5-phosphabicyclo[3.3.1]nonane-5-Oxide (DAPTA=O): synthesis, characterization and catalytic activity

Abdallah G. Mahmoud,[a],[b] M. Fátima C. Guedes da Silva,*[a] Ewelina I. Śliwa, [c] Piotr Smoleński,*[c] Maxim L. Kuznetsov [a] and Armando J. L. Pombeiro [a]

[a] *Centro de Química Estrutural, Instituto Superior Técnico, Universidade de Lisboa, Av. Rovisco Pais, 1049-001 Lisboa, Portugal. E-mail: fatima.guedes@tecnico.ulisboa.pt*

[b] *Department of Chemistry, Faculty of Science, Helwan University, Ain Helwan, 11795 Cairo, Egypt.*

[c] *Faculty of Chemistry, University of Wrocław, Ul. F. Joliot-Curie 14, 50-383 Wrocław, Poland. Email: piotr.smolenski@chem.uni.wroc.pl*

Key words: Catalysis, Catechol oxidase, Copper, DAPTA=O, Water soluble phosphanes

Abstract:

Reactions of 3,7-diacetyl-1,3,7-triaza-5-phosphabicyclo[3.3.1]nonane (DAPTA) with metal salts of Cu(II) or Na(I)/Ni(II) under mild conditions lead to the oxidized phosphane derivative 3,7-diacetyl-1,3,7-triaza-5-phosphabicyclo[3.3.1]nonane-5-oxide (DAPTA=O) and to the first examples of metal complexes based on the DAPTA=O ligand, $[Cu^{II}(\mu\text{-}CH_3COO)_2(\kappa O\text{-DAPTA=O})]_2$ (**1**) and $[Na(1\kappa OO';2\kappa O\text{-DAPTA=O})(MeOH)]_2(BPh_4)_2$ (**2**). The catalytic activity of **1** was tested for Henry reaction, as well as for the aerobic TEMPO-mediated oxidation of benzyl alcohol. Compound **1** has also been evaluated as a model system for the catechol oxidase enzyme using 3,5-di-*tert*-butyl-catechol (3,5-dtbc) as the substrate. The kinetic data fitted the Michaelis-Menten equation and enabled obtaining a rate

constant for the catalytic reaction which are among the highest obtained for this substrate using dinuclear Cu(II) complexes. DFT calculations discard a bridging mode binding type of this substrate and propose a mixed-valence Cu(II)/Cu(I) complex intermediate where the spin electron density is mostly concentrated at one of the Cu atoms and at the organic ligand.

Introduction

The interest of 1,3,5-triaza-7-phosphaadamantane (PTA) and its derivatives in transition metal coordination chemistry is dramatically increasing due to the high solubility, stability in water and far-reaching catalytic, medicinal and photoluminescent applications of the obtained compounds.[1–3] The first example of a PTA-Cu(II) complex was reported by Tu *et al*. where the metal is coordinated by a PTA-based cluster ligand.[4] Thereafter, coordination polymers based on PTA with mixed-valence Cu(I)/Cu(II) were published.[5,6] The reported examples of Cu complexes based on PTA-type ligands are mainly of Cu(I), even when Cu(II) salts were used as starting materials, due to the tendency of PTA ligands to stabilize the lower metal oxidation state.[7–10]

Among the large family of open-cage PTA derivatives,[2,11] 3,7-diacetyl-1,3,7-triaza-5-phosphabicyclo[3.3.1]nonane (DAPTA) is a relevant one (figure 1)[12,13] and its binding capacity has been intensively studied for Cu, Ru, Rh, Pd, Pt and Au transition metals to produce complexes used mainly for biological applications[14–17] and, to a lesser extent, for catalysis.[18–21] The DAPTA ligand usually exhibits the *P*-coordination mode to the metal center,[13–16,21–24] and recently the *N*-coordination mode was also reported.[18] Although DAPTA has two coordination sites from the acetyl oxygens, the *O*-coordination mode for DAPTA has not been reported yet.

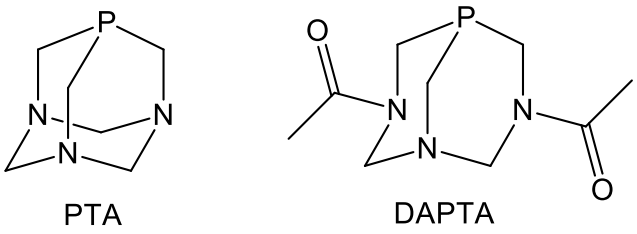

Figure 1. PTA and DAPTA

10.1002/asia.201800799

The oxidized derivatives of PTA and DAPTA, 1,3,5-triaza-7-phosphaadamantane-7-oxide (PTA=O) and 3,7-diacetyl-1,3,7-triaza-5-phosphabicyclo[3.3.1]nonane 5-oxide (DAPTA=O) were synthesized for the first time in 1977 by Siele,[12] the former upon oxidation of PTA and the latter by acetylation of PTA=O with acetic anhydride (scheme 1). Several examples are known where PTA=O binds a metal cation in the *O*-,[25,26] *N*-,[25,27] *ON*-,[25] *ONN*-,[28] *NNN*-[29] or *ONNN*- modes,[28,30] achieving either discrete metallic units or polymeric compounds. In a number of cases,[25,27] different types of coordination modes were obtained in the same molecule. For DAPTA=O, however, and despite being known for quite a long time and its structure had already been established,[12] its coordination properties have not yet been studied.

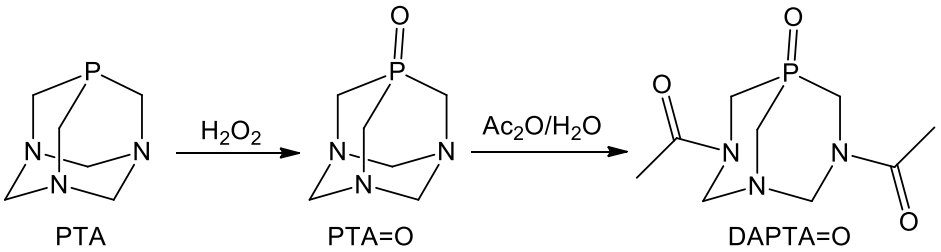

Scheme 1. Synthesis of PTA=O and DAPTA=O

Nitroaldol (Henry) reaction constitutes an important C-C bond formation reaction, accomplished by coupling nitroalkanes with carbonyl (aldehydes or ketones) compounds to produce the corresponding β-nitro alcohols (scheme 2).[31,32] These are products of great synthetic utility in view of their possible conversion into other valuable intermediates, including the reduction of the nitro group to produce β-amino alcohols,[33] oxidation to yield α-nitro ketones,[34] or dehydration to afford nitroalkenes.[35] The nitroaldol reaction can be promoted (or catalyzed) by Lewis acidic metal complexes to activate the carbonyl group, by bases to facilitate the deprotonation of nitroalkane, or both.[36–41]

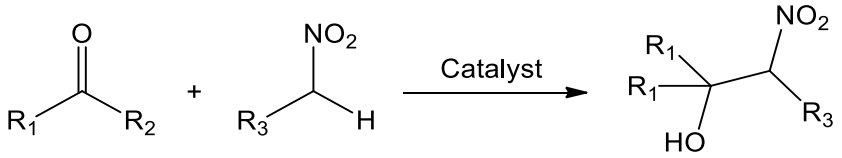

Scheme 2. Catalytic Nitroaldol (Henry) reaction (general pictogram)

The aerobic oxidation of benzylic alcohols catalyzed by transition metal salts or complexes and in the presence of the 2,2,6,6-tetramethylpiperidine-1-oxyl (TEMPO) radical is an interesting process that has been intensively studied through the last two decades, as the produced benzylic aldehydes are versatile intermediates for syntheses of other fine chemicals.[42,43]

Several copper- and other transition metal-based complexes, which effectively catalyze this reaction under different conditions, have been studied by our group.[44–47]

Among the metalloenzymes that perform the oxidation of organic compounds by activating molecular dioxygen is catechol oxidase, a type III metalloprotein that contains copper at the active center. Such enzyme has the ability to catalyze the oxidation of *ortho*-phenols to the appropriate *ortho*-quinones by molecular oxygen.[48–50] The catecholase activity of various mono- and dicopper compounds, as well as copper clusters with different structural topologies, has been widely explored.[49–60]

In this work we aimed to pursue our interests on the coordination chemistry of PTA and derivatives,[5–10,14,26,28,61–64] chaining the aforementioned lines towards: i) the synthesis and characterization of hydrosoluble transition metal complexes containing DAPTA or DAPTA=O, the coordination chemistry of which is virtually unexplored; ii) the understanding of the experimental conditions for the DAPTA oxidation to DAPTA=O; iii) the study of the catalytic properties of the obtained copper(II) complex, $[Cu^{II}(\mu\text{-}CH_3COO)_2(\kappa O\text{-DAPTA=O})]_2$ (**1**), towards nitroaldol (Henry) reaction and alcohols oxidation in water as reaction medium, as well as, iv) the study of the biomimetic behaviour of this copper complex towards catechol oxidation.

Results and Discussion

Synthesis and characterization of complexes 1 and 2

The DAPTA=O ligand has been formed spontaneously by a one-pot simple reaction of DAPTA with metal salts in air under mild conditions (scheme 3). The dinuclear air-stable Cu(II) complex $[Cu(\mu\text{-}CH_3COO)_2(\kappa O\text{-DAPTA=O})]_2$ (**1**) was obtained by reaction of Cu(II) acetate monohydrate with DAPTA under air and at room temperature (route1, scheme 3) and

stemmed from oxidation of DAPTA, presumably with concomitant reduction of Cu(II) resulting in the *O*-bound DAPTA=O Cu(II) complex **1**. This complex exhibits a high solubility in water, dimethyl sulfoxide, methanol, ethanol, acetonitrile and dichloromethane, whereas it is not soluble in diethyl ether and hexane.

The addition of $Na(BPh_4)$ to a methanolic solution of DAPTA in air at room temperature and in the presence of nickel acetate hexahydrate led to the formation of the dinuclear sodium complex $[Na(\mu\text{-}1\kappa OO';2\kappa O\text{-DAPTA=O})(MeOH)]_2(BPh_4)_2$ (**2**) as a white air-stable solid (route 2, scheme 3). The reaction also involved the oxidation of DAPTA and the presence of a Ni(II) salt proved to be essential for the formation of **2**. Complex **2** exhibits a high solubility in water, dimethyl sulfoxide and methanol, but it is not soluble in other common solvents.

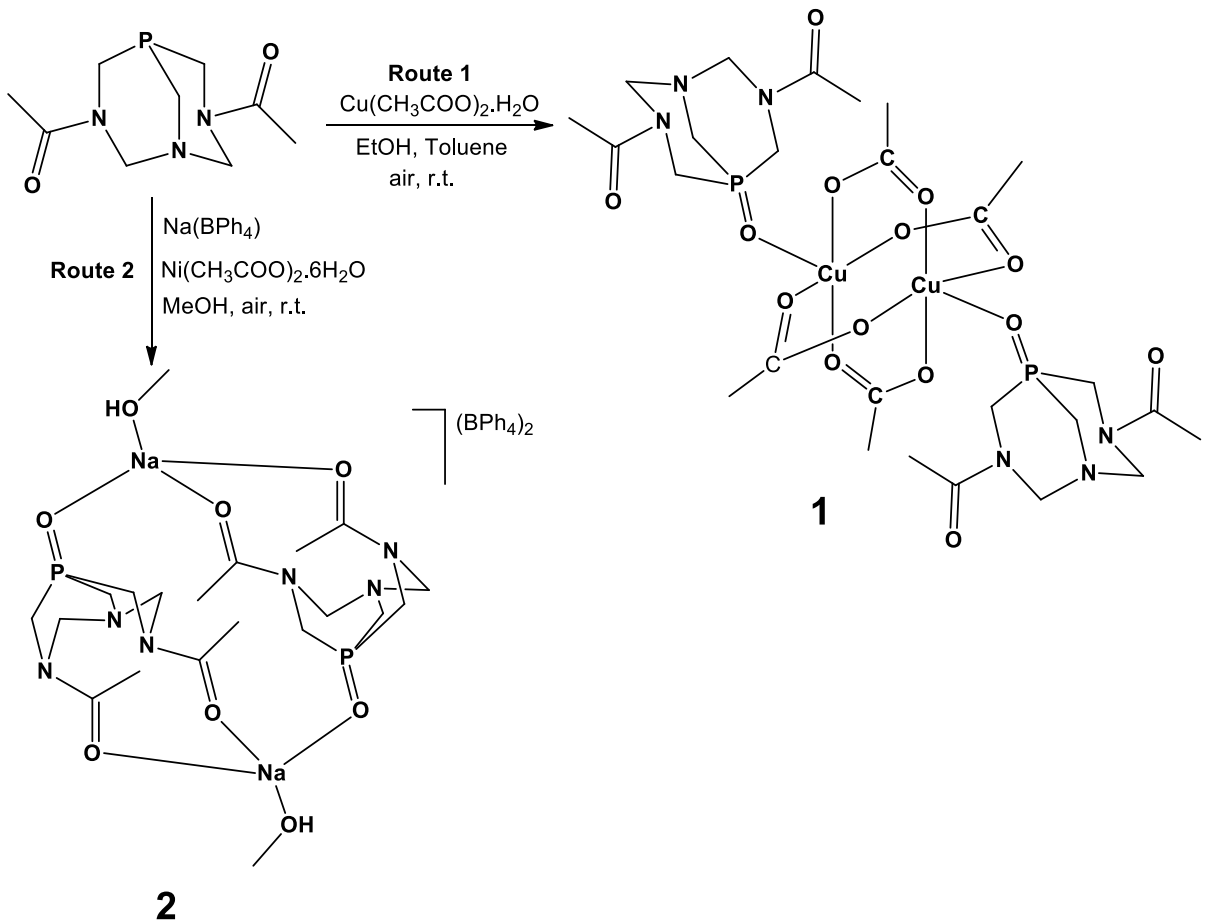

Scheme 3. Synthetic procedures for DAPTA=O metal complexes

Compounds **1** and **2** were characterized by elemental analysis, ESI(+)-MS, FT-IR, ^1H and $^{31}P\{^1H\}$ NMR spectroscopies and single-crystal X-ray diffraction analysis. The IR spectra of

the complexes exhibit ν(P=O) at 1153 (**1**) and 1163 (**2**) cm^{-1}, as well as ν(C=O) at 1627 (**1**) and 1631 (**2**) cm^{-1}, which are close to the typical values of free phosphane oxide [ν(P=O) at 1190 cm^{-1} and ν(C=O) at 1615].[12] Despite the paramagnetism of **1**, its ^{1}H and ^{31}P NMR spectra showed the signals corresponding to DAPTA=O fragments, although with the ^{1}H signals slightly broadened. The observation of NMR resonances in paramagnetic compounds have been reported and attributed to the ligands remote locations from the paramagnetic metal ions.[4–6] The ^{1}H NMR spectra of **1** and **2** display similar resonances for the acyl methyl groups and methylene protons compared to the free DAPTA.[22] For both compounds, the sole acyl methyl resonances in the ^{1}H NMR spectra indicates their equivalent environment. The splitting patterns assigned to the methylene NCH_2N and PCH_2N protons (3.5-5.8 ppm) are indicative of their diastereotopicity, also revealing the coupling of all PCH_2N protons to the phosphorus nucleus.[22] The sharp singlets at δ 2.95 (**1**) or 3.10 (**2**) in the $^{31}P\{^{1}H\}$ NMR spectra are slightly downfield from the resonance of free DAPTA=O (2.20 ppm).[13]

Adventitious water seems to play a crucial role for DAPTA oxidation and the formation of compounds **1** and **2**, since they could not be obtained using dry solvents and under strict inert conditions, despite the presence of some water in the metal salts. They could be formed, however, by performing the reactions in undried degassed solvents, using Schlenck techniques and under N_2 atmosphere.

The role of water in such an oxidation process has already been reported by Frost *et al*.,[25] for related systems where DAPTA is oxidized to DAPTA=O + $2H^{+}$. In our case, this oxidation process is presumably combined with the reduction of Cu(II) (route1, scheme 3) or Ni(II) (route 2, scheme 3). To prove the role of water in the DAPTA oxidation process, the synthesis of **1** was undertaken under inert N_2 atmosphere, using freshly dried solvents and ^{18}O-labeled water ($H_2{}^{18}O$) in the reaction medium (see experimental part). The obtained material was analysed using ESI(+)-MS, and the spectrum reveals a set of fragments attributable to DAPTA=O^{18} (see experimental part and figure S1).

X-ray diffraction analysis. Compounds **1** and **2** crystallize in the triclinic space group and are both dimeric with their asymmetric units containing only half of the molecules, *viz.* a Cu(II) cation *O*-bound by two acetate and one DAPTA=O ligands in **1**, and a Na(I) cation *O*-bound by a chelating DAPTA=O and a methanol molecule in **2**, the latter also containing a tetraphenylborate counter-ion. The second halves of the molecules are generated by

10.1002/asia.201800799

symmetry (figure 2) and give rise to ring-type neutral (in **1**) or cationic (in **2**) dinuclear units. While in **1** the metal cations are gathered by means of four bridging chelate acetate anions, in **2** the metal cations are connected solely via the oxidized phosphane moiety which, overall, acts as a three *O*-donor ligand. Thus, the copper atoms in **1** assume perfect all-*O* square pyramidal geometries (τ_5 = 0.00)[65] and the sodium atoms in **2** display distorted all-*O* tetrahedral ones (τ_4 = 0.77).[66] In **1** the metals are involved in just one type of metallacycle, an 8-membered $C_2Cu_2O_4$ ring, but the sodium cations in **2** are engaged in 14-, 16- and 18-membered metallacycles of the type $C_xN_yNa_2O_4P_2$ (x = 4 or 6; y = 2 or 4). In both structures the metals, the P and the $O_{phosphane}$ atoms lie in the same plane. In **1** no other atoms can be included in such plane, while in **2** it also contains the amine N1 and the methylene C1 atoms. The Cu–$O_{acetate}$ bond distances in **1** (table 1) are close to each other and shorter than the Cu–$O_{phosphane}$ [*avg*. 1.964(3) and 2.182(2) Å, respectively]; in **2** the Na–$O_{phosphane}$ is the shortest metal–O length [2.207(3) Å] followed by the Na–$O_{methanol}$ bond [2.274(3) Å], the Na–O_{acetyl} being the longest [2.285(3) and 2.329(3) Å]. The P–$O_{phosphane}$ distances are of 1.490(3) Å in **1** and of 1.473(2)Å in **2**. The metal···metal intramolecular distances adopt values of 2.612 (**1**) and 6.996 Å (**2**), but the minimum intermolecular ones assume values of 7.515 and 7.216 Å (in **1** and **2**, respectively).

The BPh_4 anion in **2** appears to play an important role in the stabilization of the structure in view of the short C(or O)–H···π interactions concerning DAPTA=O (or methanol) ligand as donor, which range from 2.49 to 2.96 Å. In addition, the observed intermolecular contacts between the sodium cations and the C12, C13 and C14 aromatic carbons of the BPh_4 anion, with minimum distance of 3.182 Å pertaining to C13, may account for the distortion of the tetrahedral environment in dimer **2**.

10.1002/asia.201800799

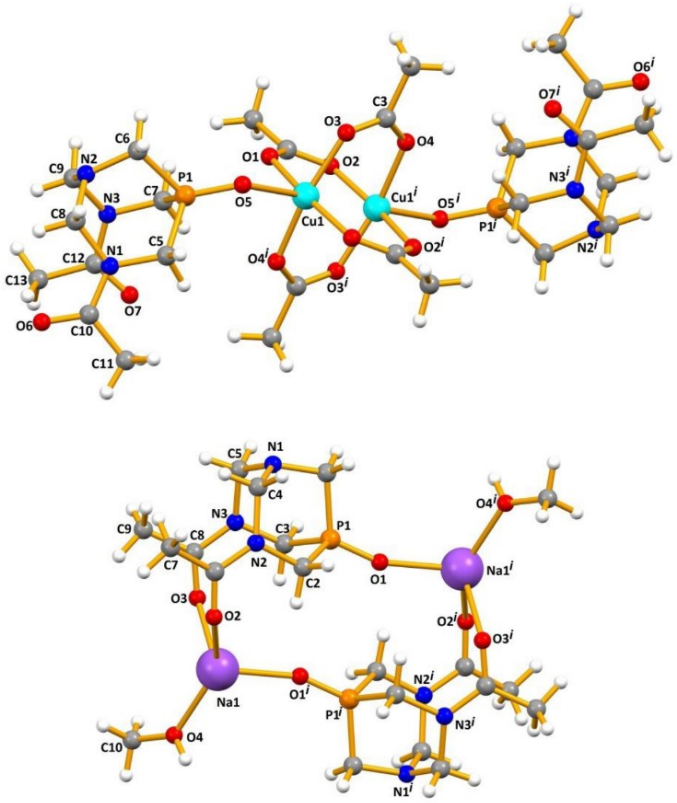

Figure 2. The molecular structures of **1** (top) and **2** (bottom) with partial atom labelling schemes. The BPh_4 counter-ions of **2** are omitted for clarity. Symmetry operations to generate the *i* equivalent atoms: 1-x,-y,1-z (**1**) and 2-x,2-y,1-z (**2**).

Table 1. Selected bond distances (Å) and angles (°) for **1** and **2** [a]

1		**2**	
O1–Cu1	1.969(3)	O1–Na1^i	2.207(3)
O2–Cu1^i	1.956(3)	O2–Na1	2.285(3)
O3–Cu1	1.964(3)	O3–Na1	2.329(3)
O4–Cu1^i	1.965(3)	O4–Na1	2.274(3)
O5–Cu1	2.182(2)	O1–P1	1.473(2)
O5–P1	1.490(3)	O1–Na1–O4^i	110.84(13)
Cu1–Cu1^i	2.6117(9)	O1–Na1–O2^i	103.49(10)
P1–O5–Cu1	128.66(14)	O4–Na1–O2	140.04(12)
O3–Cu1–O1	90.36(11)	O1–Na1–O3^i	101.20(11)
O3–Cu1–O5	96.76(10)	O4–Na1–O3	105.84(12)

O1–Cu1–O5	94.22(10)	O2–Na1–O3	86.36(9)

[a] See figure 2 legend for the symmetry codes

Catalytic activity of complex 1

Nitroaldol (Henry) reaction. Under mild conditions and in air, complex **1** was tested as homogeneous catalyst for nitroaldol coupling of benzaldehyde with nitromethane and nitroethane (see above and scheme 2) in aqueous medium. The optimization of the reaction conditions was attained by exploring some experimental variables such as reaction time and temperature.

Table 2 displays the results of the reaction of benzaldehyde with nitromethane to give 1-phenyl-2-nitroethanol. By using 5 mol% of the catalyst, at 75 ^{o}C, the product yield increased with time up to 94 % after 60 h (table 2, entries 1-9 and figure 3). No significant increase in the yield was observed by extending the reaction time to 72 h. Using ethanol (another protic solvent) gave higher yields than when using water for the same period of time (table 2, entries 10 and 12: 97 against 87 %, both at 60 ^{o}C). A 1:1 mixture of ethanol and water gave an yield (96 %) identical to that when using ethanol alone (table 2, entry 11). It was also observed that in water as the sole solvent, the conversion increased with the increase of temperature up to 91% after 48 h (table 2, compare entries 8, 12, 13 and 14). In the presence of a base (triethylamine), in water and for 24 h at room temperature, the conversion was quantitative (table 2, entry 15). In the absence of **1** but in the presence of any of several Cu(II) salts, only 12 to 38 % of conversion was achieved after 24 h at 75 ºC (table 2, entries 16-19).

Table 2. Henry reaction of nitromethane with benzaldehyde using complex **1** as catalyst [a]

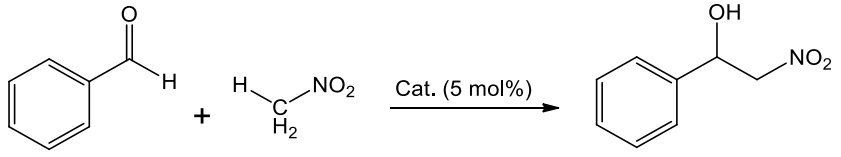

Entry	Catalyst	Time (h)	T (^{o}C)	Solvent	Yield [b] (%)	TON [c]
1	**1**	2	75	Water	7	2
2	**1**	4	75	Water	15	3
3	**1**	6	75	Water	21	4
4	**1**	8	75	Water	38	8

5	**1**	12	75	Water	45	9
6	**1**	24	75	Water	69	14
7	**1**	36	75	Water	87	18
8	**1**	48	75	Water	91	18
9	**1**	60	75	Water	94	19
10	**1**	48	60	Ethanol	97	20
11	**1**	48	60	Water:Ethanol (1:1)	96	19
12	**1**	48	60	Water	87	18
13	**1**	48	23	Water	72	15
14	**1**	48	50	Water	87	18
15 [d]	**1**	24	23	Water	>99	20
16	$CuSO_4.5H_2O$	24	75	Water	12	2
17	$Cu(OAc)_2.H_2O$	24	75	Water	38	8
18	$CuCl_2.2H_2O$	24	75	Water	18	4
19	$Cu(NO_3)_2.2.5H_2O$	24	75	Water	26	5

[a] Reaction conditions: benzaldehyde (0.5 mmol), 5 mol% of catalyst, 3 equiv of nitromethane (1.5 mmol), 2 mL of solvent. [b] Determined by ^{1}H NMR analysis of the crude products (see Experimental part and figure S2). [c] Number of moles of the product (1-phenyl-2-nitroethanol) per mol of catalyst. [d] In the presence of 5 mol% triethylamine.

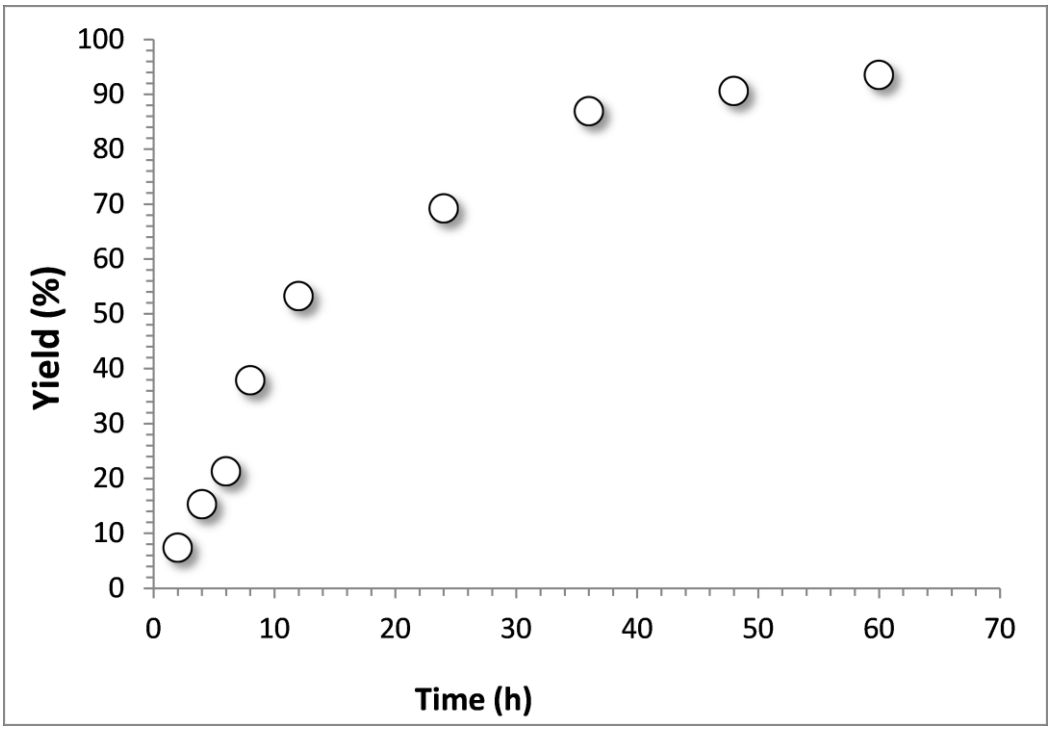

Figure 3. Variation of the product yield with time in the reaction between benzaldehyde and nitromethane catalysed by **1.**

The nitroaldol catalyzed reaction was also performed using nitroethane instead of nitromethane, affording the *anti* and the *syn* diastereoisomeric forms of 1-phenyl-2-

10.1002/asia.201800799

nitropropanol (table 3). In aqueous medium, using catalytic amounts of **1** at 75 ^{o}C, a maximum yield of 88 % is achieved in 60 h with a higher selectivity towards the *syn* isomer (table 3, entries 1-5).

As indicated above, using a catalytic amount of a base (5 mol% of triethylamine) led to an improvement in the reaction yield (87 %) in a shorter time and at room temperature (table 3, entry 6), although in this case with a decrease in selectivity.

The catalytic study of complex **1** for nitroaldol reaction was extended to various *para*-substituted aromatic aldehydes (table 4). With both nitroalkanes, the corresponding β-nitroalcohols were obtained with yields ranging from 51 % to 97 %, with higher selectivity towards the *syn* isomer when nitroethane was used. The results indicate that an aromatic aldehyde bearing an electron-withdrawing group (nitro, bromo or chloro, table 4, entries 7-12) exhibits a higher reactivity than those with electron-donating substituents (methoxy or methyl, table 4, entries 1-4), which is due to the higher electrophilicity of the aldehyde group in the first case.

Table 3. Henry reaction of nitroethane with benzaldehyde using complex **1** as catalyst [a]

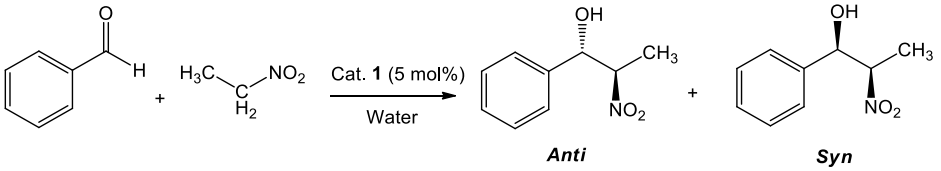

Entry	Time (h)	T (^{o}C)	Yield [b] (%)	Selectivity [b] (*anti* : *syn*)	TON [c]
1	12	75	37	28 : 72	7
2	24	75	48	23 : 77	10
3	36	75	66	27 : 73	13
4	48	75	83	30 : 70	17
5	60	75	88	29 : 71	18
6 [d]	24	23	87	49 : 51	18

[a] Reaction conditions: benzaldehyde (0.5 mmol), 5 mol% of catalyst, 3 equiv of nitroethane (1.5 mmol), 2 mL of solvent. [b] Determined by ^{1}H NMR analysis of crude products (see Experimental part and figure S3). [c] Number of moles of product (1-phenyl-2-nitropropanol) per mol of catalyst. [d] In the presence of 5 mol% triethylamine.

Table 4. Henry reaction of nitroalkanes with various aldehydes using complex **1** as catalyst [a]

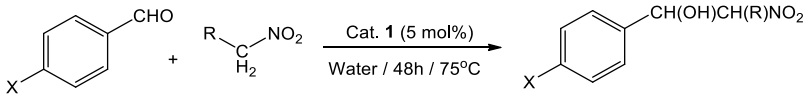

Entry	X	R	Yield [b] (%)	Selectivity [b] (*anti* : *syn*)	TON [c]
1	MeO	H	51	-	10
2		Me	51	32 : 68	10
3	Me	H	81	-	16
4		Me	80	33 : 67	16
5	H	H	91	-	18
6		Me	83	30 : 70	16
7	NO_2	H	97	-	20
8		Me	91	42 : 58	18
9	Br	H	95	-	19
10		Me	88	29 : 71	18
11	Cl	H	92	-	18
12		Me	84	36 : 64	17

[a] All reactions were performed at 75^{o}C for 48 h in air, using 0.5 mmol of aldehyde with 5 mol% of catalyst and 3 equiv. of nitroalkane (1.5 mmol) in 2 mL of water. [b] Determined by ^{1}H NMR analysis of crude products (see Experimental part and figure S4). [c] Number of moles of the produced β-nitro alcohol, per mol of catalyst.

Since complex **1** has a metal-acetate type structure, the mechanism of the reaction is expected to be similar to that reported by Evans *et al.* for related catalytic systems,[67] where the Lewis acidic copper(II) centers of **1**, bearing moderately basic charged acetate ligands, would facilitate the nitroalkane deprotonation as a prelude to the aldol addition step. It would also activate the aldehyde moiety towards nucleophilic attack by the nitronate species $R(NO_2)CH^-$.[36]

In comparison to the few examples found in literature for catalytic nitroaldol reaction in aqueous medium using catalysts based on different transition metals (table S1), the yields observed in this work are found to be comparable or even better in some cases, taking into consideration the reaction conditions such as temperature, amount of catalyst and reaction time.[36,37,68–73]

Aerobic oxidation of benzyl alcohol. Compound **1** was also tested as catalyst for the aerobic oxidation of benzyl alcohol mediated by TEMPO (2,2,6,6-tetramethylpiperidine-1-oxyl radical) in aqueous medium to give benzaldehyde (table 5). Performing this reaction for 6 h at room temperature using 5 mol% of **1** and TEMPO, gave only 16 % yield on benzaldehyde (Table 5, entry 1). Increasing the temperature to 80 ^oC rose the yield up to 41 % in 6 h (table 5, entry 2), and an extension of the reaction time, keeping this latter temperature, led to a significant improvement of the yield (78 % after 21 h and 89 % after 48 h: table 5, entries 3 and 4). In agreement with what has already been reported,[44–47] the presence of a base (K_2CO_3) and of TEMPO are crucial for the reaction to proceed (table 5, entries 5 and 6).

The catalysis mechanism is expected to be similar to the one previously proposed for a Cu(II)-TEMPO-air radical catalytic system.[74,75] The TEMPO radical and base-assisted deprotonated alcohol (RCH_2O^-) coordinate to the Cu(II) center which simultaneously activates these species. Hydrogen abstraction of the alcoholate α-carbon by TEMPO occurs, the resulting *O*-ligated $RC^{\bullet}HO^-$ radical being stabilized by H-bond. The following intramolecular electron transfer from the bound radical to the Cu(II) center produces the aldehyde (RCHO), TEMPO-H and a Cu(I) species which is thereafter TEMPO-mediated reoxidized to Cu(II).

Table 5. Aerobic oxidation of benzyl alcohol to benzaldehyde using complex **1** as catalyst [a]

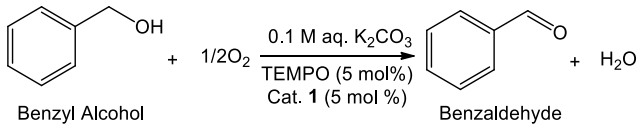

Entry	Time (h)	Temp. (°C)	Yield [b] (%)	TON [c]
1	6	23(RT)	16	3
2	6	80	41	8
3	21	80	78	16
4	48	80	89	18
5 [d]	6	80	14	3
6 [e]	6	80	<1	-
7 [f]	6	80	<1	-

[a] All reactions were performed in open air using 0.5 mmol of benzyl alcohol, 5 mol% of catalyst **1** and 5 mol% of TEMPO in 2 mL of 0.1 M K_2CO_3 aqueous solution. [b] Calculated using GC analyses. [c] Number of moles of the product benzaldehyde, per mol of catalyst. [d] In water without K_2CO_3. [e] Without TEMPO. [f] Without the metal catalyst.

Catecholase activity. The catalytic activity of compound **1** was also investigated in the oxidation of 3,5-di-*tert*-butyl-catechol (3,5-dtbc) to the corresponding diketone 3,5-di-*tert*-butyl-quinone (3,5-dtbq) under aerobic conditions as a model reaction (scheme 4). This substrate has been broadly used because of the low redox potential for the quinone-catechol couple (easy oxidation to the corresponding quinone) and of the bulky substituents which inhibit degradation of the substrate for at least 6 h.[76]

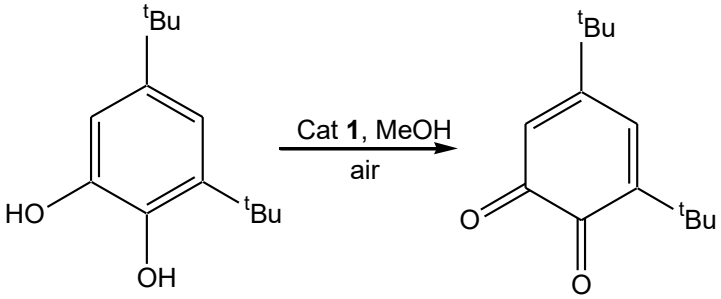

Scheme 4. Schematic representation of the oxidation of 3,5-dtbc to 3,5-dtbq

The product is stable and the UV-Vis spectrum in methanol shows an intense band at 390 nm with $\varepsilon = 1518\ M^{-1}cm^{-1}$ (see figure S5). The absorption at 390 nm was measured as a function of time over the first 5 min. In figure 4 it is observed the growth of the quinone band during the reaction.

10.1002/asia.201800799

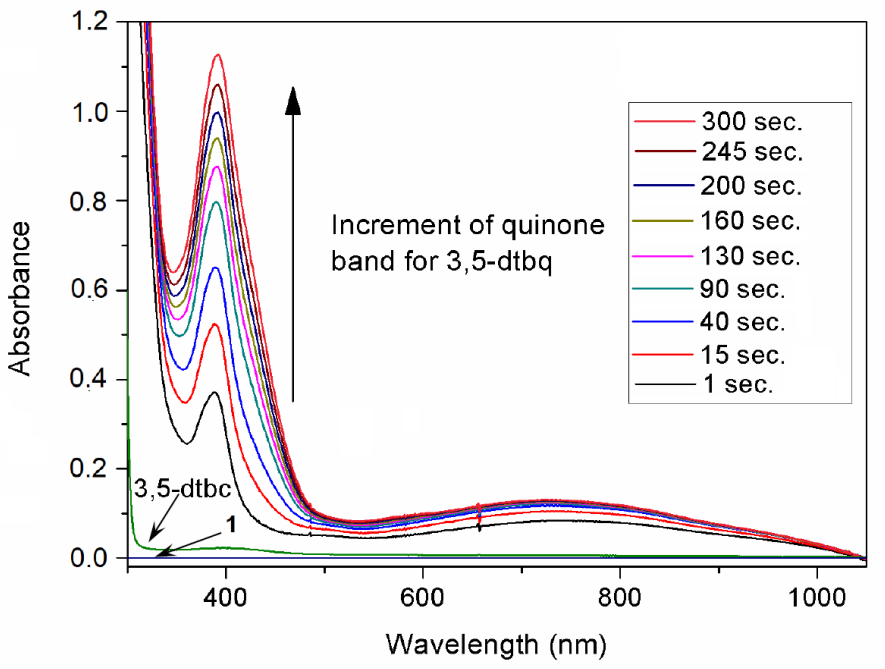

Figure 4. Increase of quinone band at 390 nm after addition of compound **1** (6.57×10^{-5} M) to a solution of 3,5-dtbc (1.35×10^{-2} M) in methanol at 25 °C

To determine the rate dependence on the substrate concentration, a solution of compound **1** was treated with different concentrations of 3,5-dtbc. The kinetic study was carried out using the initial slope method. The rates of the reactions for different substrate concentrations was fitted to the Michaelis-Menten equation (figure 5). On the basis of the obtained data, a rate constant (k_{cat}) of 50.8 min^{-1} was obtained, the maximum rate (V_{max}) achieved was of $3.34 \times 10^{-3} \pm 3.55 \times 10^{-5}$ M min^{-1} and a Michaelis constant (K_M) of $1.14 \times 10^{-4} \pm 9.21 \times 10^{-6}$ M ($R^2 = 0.93566$), therefore leading to a catalytic efficiency (k_{cat}/K_M) of 4.46×10^5 $M^{-1}min^{-1}$.

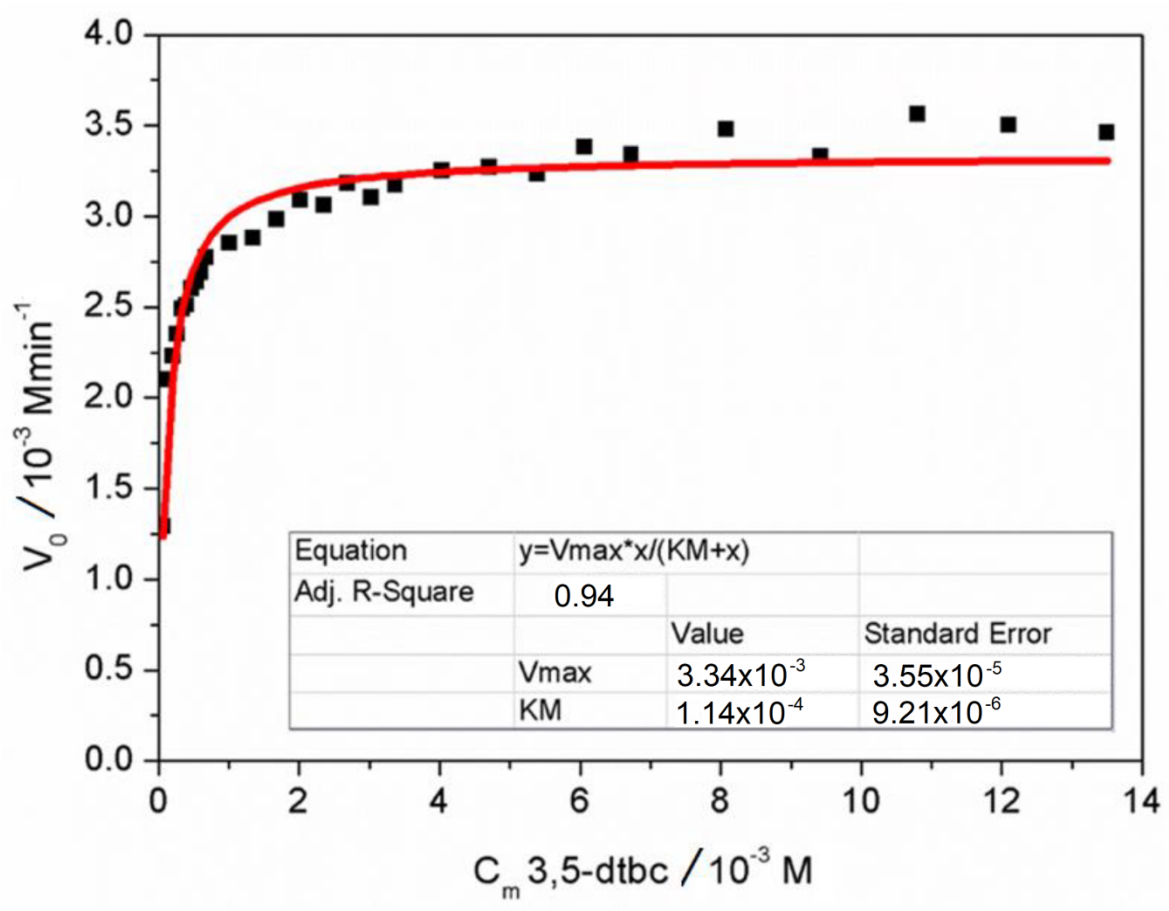

Figure 5. Michaelis-Menten plot for the oxidation of 3,5-dtbc (concentration range: 6.73×10^{-5} – 1.35×10^{-2} M) catalyzed with complex **1** (6.57×10^{-5} M) in methanol at 25 °C.

The obtained value for the kinetic parameter is significantly higher than those reported for other dinuclear Cu(II) compounds containing acetate ligands,[51,52,59,60] as well as for other copper(II) compounds.[76–78] However, our k_{cat} value is much lower than that found, *e.g.* for the cationic compound $[Cu_2(H_2L)(OH)(H_2O)(NO_3)](NO_3)_3$ (L = 2,6-bis(*N*-ethylpiperazine-iminomethyl)-4-methyl-phenolato), for which k_{cat} was 540 min^{-1},[79] but the catalytic efficiency of this catalyst is shorter (2.35×10^5 $M^{-1}min^{-1}$) than that observed for **1** (see above). It has been suggested that the geometry around the copper ions and the electronic features of the complex determine its catecholase-like activity, with square-planar complexes commonly being the most active ones.[60] In the case of **1** the change of bidentate to monodentate coordination of two acetate bridging ligands can allow the coordination of 3,5-debc in the usually proposed bridging mode between the two Cu(II) ions. The rate of this catalytic reaction has been tentatively related, among other parameters, with the Cu···Cu separation in

10.1002/asia.201800799

the catalyst molecule: the larger this distance, the lower the reaction rate since the bridging of the substrate between the metals is consequently hampered.[53] In this respect, the distance of 2.612 Å between the two metals in **1** is much shorter than that of *ca*. 2.9 Å considered as appropriate for a copper catalyst mimicking catechol oxidase.[60] Contrary to what was found for other dicopper-based catalysts where rigid frameworks are usually met together with good electron donor bridging ligands such as phenoxide,[60] the two metals in **1** are hold solely by acetate anions, with DAPTA=O eventually playing a stabilizing role of both the oxidized and reduced states of copper.

In line with what has been proposed,[60,80] the 3,5-dtbc oxidation can involve (scheme 5) a transient semiquinone radical and the Cu(II)-to-Cu(I) reduction of the metal centers; the presence of dioxygen, would lead to the regeneration of the dicopper(II) catalyst **1**.

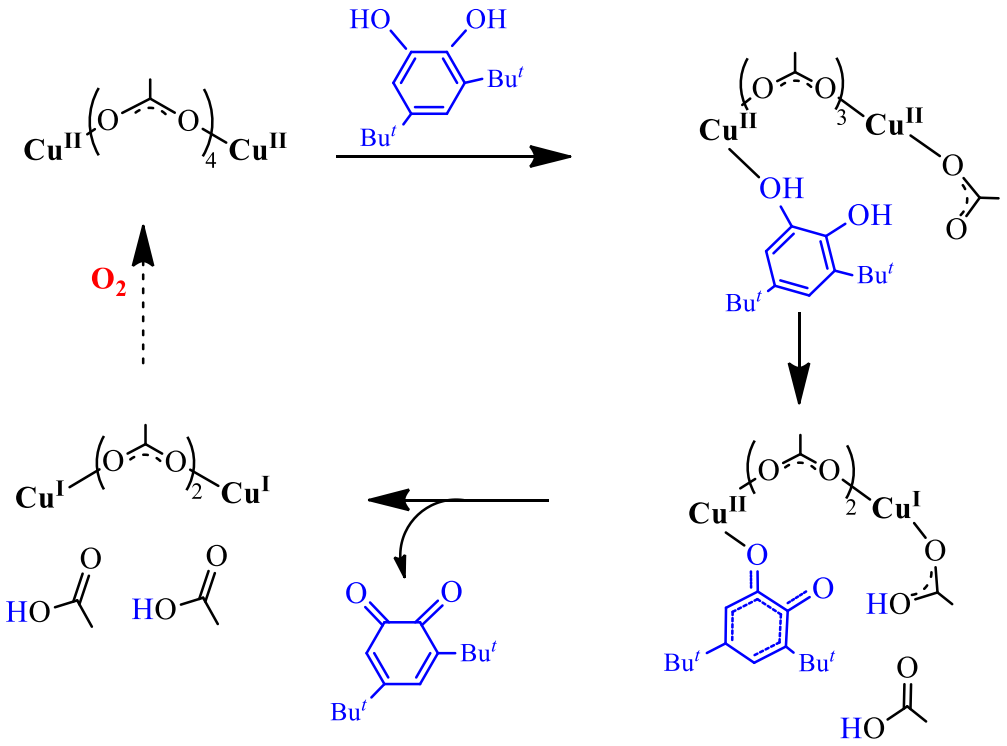

Scheme 5. Proposed general mechanism of 3,5-dtbc oxidation catalyzed by complex **1** (the DAPTA=O ligands were omitted for clarity).

Theoretical studies. With the aim to support the proposed catalytic cycle, theoretical DFT calculations of the crucial steps of the catechol oxidation catalysed by the model complex $[Cu(\mu\text{-}CH_3COO)_2(OPH_3)]_2$ (**1'**) in triplet spin state have been carried out. Since the

10.1002/asia.201800799

coordination spheres of the copper atoms in the catalyst molecule are saturated, the ligation of catechol to the metal center(s) requires the formation of a free coordination site. This may occur upon protonation of one acetate ligand in **1'** by catechol to give intermediate **3** followed by the elimination of acetic acid leading to complex **4** (scheme 6). However, the energy of the proton transfer from catechol to the acetate ligand is very high (43.6 kcal/mol), and this pathway may be ruled out.

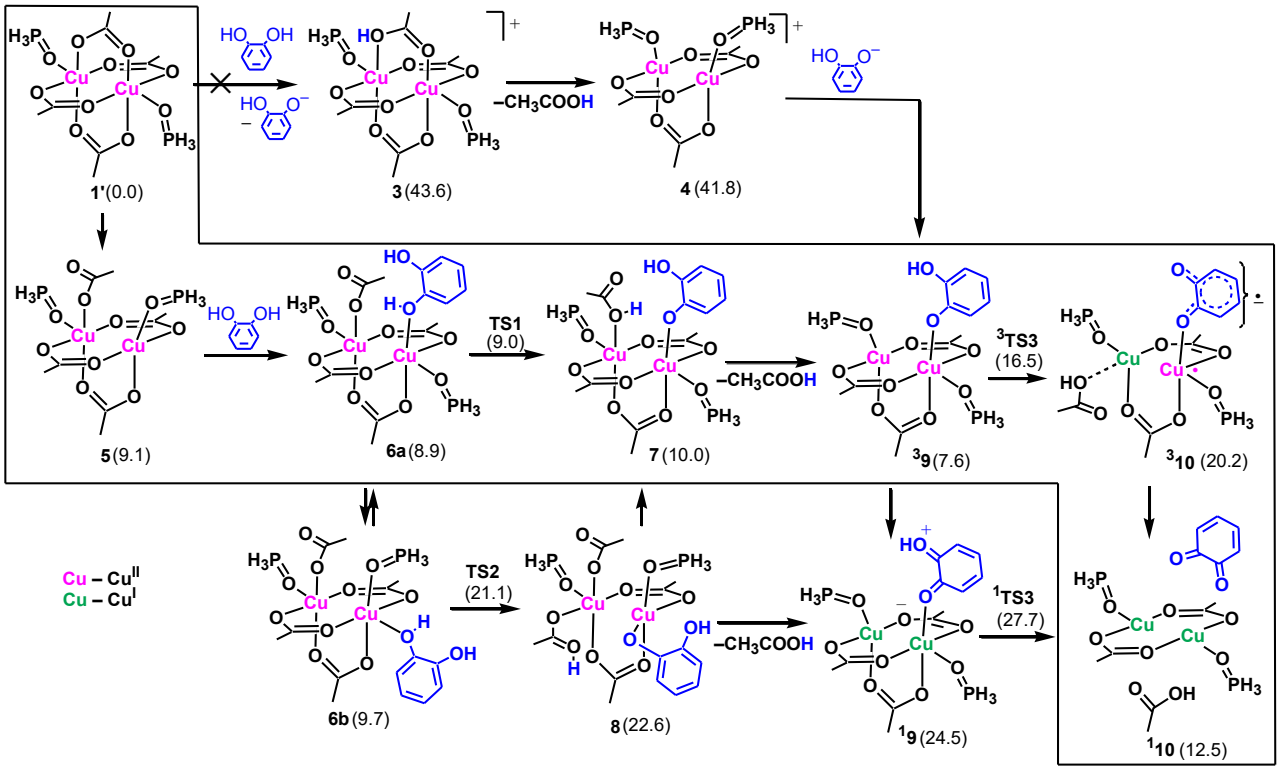

Scheme 6. Mechanisms of the catechol oxidation catalyzed by the model complex **1'**. The Gibbs free energies in methanol solution are indicated in kcal/mol relative to **1'** + catechol. The most favorable mechanism is boxed.

Another possibility is decoordination of an acetate ligand from one of the copper atoms to give complex **5**. This process requires only 9.1 kcal/mol (in terms of ΔG_s). The ligation of catechol to **5** is almost energetically neutral (ΔG_s = –0.2 kcal/mol) and results in the formation of complex **6**. For the latter, two isomers with different positions of the catechol ligand were found, **6a** and **6b** (scheme 6), but with similar energies. The proton transfer from the catechol ligand to an acetate ligand in **6a** or **6b** leads to the hydrocatecholate Cu(II)/Cu(II) complexes **7** or **8**, respectively. The H-transfer in **6a** occurs via transition state

10.1002/asia.201800799

TS1 with very low activation energy of 0.1 kcal/mol. The H-transfer in **6b** via **TS2** requires a much higher barrier of 11.4 kcal/mol and, therefore, this pathway may be excluded from the following consideration.

Gibbs free energies of both **TS1** and **TS2** are slightly lower than the energies of the reaction products **7** and **8**, respectively. This may be explained by the fact that the equilibrium geometries of all calculated species correspond to minima on the enthalpy (0 K) surface rather than on the Gibbs free energy surface. Indeed, in terms of the enthalpy at 0 K, the energies of both transition states are higher than the energies of the corresponding products (table S2).

The monodentate acetic acid in **7** may be easily eliminated affording ^{3}**9** (ΔG_s = –2.3 kcal/mol). In structure ^{3}**9**, the hydrocatecholate ligand is coordinated to only one of the Cu atoms, and thus a bridging bidentate type of the hydrocatecholate ligand was not found.

The following transformation of the hydrocatecholate into quinone may occur via two possible routes. The first one includes a proton transfer from the hydrocatecholate ligand to one of the acetates in ^{3}**9** via ^{3}**TS3** and, after acetic acid elimination, leads to the triplet complex ^{3}**10**. In this complex, spin electron density is mostly concentrated at one of the Cu atoms and at the organic ligand (figure 6) indicating that this is a mixed valence Cu(II)/Cu(I) complex and that the proton shift in ^{3}**9** results in the intramolecular single-electron oxidation of catechol to semiquinone by one of the metal centers. The second single-electron oxidation of the semiquinolate ligand in ^{3}**10** to the quinone product occurs upon spontaneous spin conversion to the singlet closed shell Cu(I)/Cu(I) complex ^{1}**10** with both acetic acid and quinone molecules being in the second coordination sphere (ΔG_s = 7.7 kcal/mol).

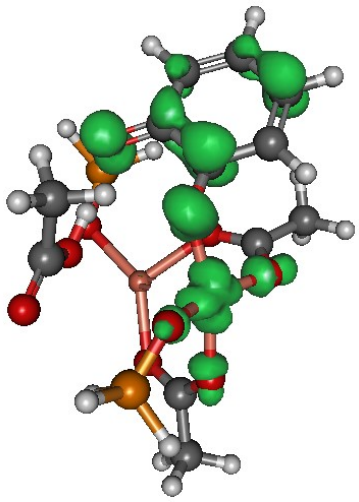

Figure 6. Spin density distribution in ^{3}**10**.

The next pathways include the excitation of complex ^{3}**9** into the singlet spin state followed by the proton transfer via the singlet ^{1}**TS3** to yield the quinone complex ^{1}**10**. This pathway is associated with the activation barrier of 27.7 kcal/mol that is too high for a reaction easily occurring at room temperature.

The most plausible mechanism of the catechol oxidation can be described by the following sequence of the reaction steps: **1'** → **5** (+ catechol) → **6a** → **7** → ^{3}**9** (–CH_3COOH) → ^{3}**10** → ^{1}**10** (scheme 6). The calculated overall Gibbs free energy of activation for the catechol oxidation is 16.5 kcal/mol, and ^{3}**TS3** is the rate limiting transition state. Such rather low activation barrier correlates with the experimental data on the rapid conversion of 3,5-tdbc at room temperature.

Conclusions

Two dinuclear hydrosoluble complexes of Cu(II) and Na(I) are reported, which constitute the first examples of metal complexes containing DAPTA=O as ligands. The oxidized phosphane ligand was prepared in a one-pot simple reaction of DAPTA in an undried solvent, in the presence of a metal salt in air under mild conditions. Based on the results obtained by deliberately using ^{18}O-labeled water, the source of oxygen in the DAPTA=O ligand was proved to be this solvent, adventitiously present in the reaction mixture. Of interest is that the Na(I) complex **2** represents the first case of DAPTA core *O*-coordination ability through the oxygen atoms of the acetyl groups.

The Cu(II) complex **1** was proved to be a moderately active catalyst not only for the Henry reaction but also for the aerobic alcohol oxidation, using water as solvent. Moreover, compound **1** has been successfully evaluated as a model for the catechol oxidase enzyme by using 3,5-di-*tert*-butyl-catechol (3,5-dtbc) as substrate, showing one of the highest activities (as measured by the catalytic rate constant k_{cat} of 50.8 min^{-1}) and one of the highest catalytic efficiencies (determined by the k_{cat}/K_M ratio of 4.46 × 10^5 $M^{-1}min^{-1}$), as compared to other previously described dinuclear acetate-bridging copper(II) complexes.

Theoretical DFT calculations revealed that the most plausible mechanism of the catechol oxidation into quinone catalysed by the diphosphinoxido tetraacetate dicopper(II) complex

includes the decoordination of an acetate ligand from one of the Cu centers in the catalyst molecule and ligation of the catechol molecule to the formed vacant coordination site, then followed by proton transfer from the catechol to the monodentate acetate and elimination of acetic acid; a second proton transfer from the hydrocatecholate ligand to an acetate ligand and spin conversion of the formed product gives the final quinone and a Cu(I)/Cu(I) complex. The proposed mechanism involves, therefore, a mixed valence Cu(II)/Cu(I) species and the cooperation of the acetate ligand. Despite the dinuclear character of the catalyst, during the oxidation process the catechol substrate appears to interact directly with only one of the metal centers.

The study demonstrates for the first time that DAPTA=O can behave as a convenient ligand under various viewpoints: i) it imparts water solubility to its complexes, allowing their use in water, *e.g.* as catalysts; ii) it assists the metal center, Cu(II), to acquire suitable electronic properties for Lewis acid and oxidation catalysis; iii) it conceivably provides stereochemical protection of the metal center, assisting its stabilization along the reaction. Therefore, the coordination chemistry of this still virtually unexplored ligand deserves to be further explored, namely in fields of Lewis acid and redox catalysis in aqueous medium.

Experimental Section

Materials and Methods. Starting materials (copper acetate monohydrate, nickel acetate hexahydrate, sodium tetraphenylborate, 3,5-di-*tert*-butylcatechol and 3,5-di-*tert*-butylquinone) and solvents were obtained from commercial sources and used as received without further purifications. DAPTA was synthesized by following an already published procedure,[12,13] and all synthetic work was performed in air.

Carbon, hydrogen and nitrogen elemental analyses were carried out by the Microanalytical services of the Instituto Superior Técnico. Fourier transform infrared (FTIR) spectra (4000–400 cm^{-1}) were recorded on a Bruker Vertex 70 instrument as KBr pellets. ^{1}H and ^{31}P NMR spectra were measured at ambient temperature using Bruker Avance 300 or 400 MHz spectrometers. All chemical shifts are quoted in δ (ppm). ^{1}H NMR spectra were referenced internally to residual protio-solvent resonance and are reported relative to tetramethylsilane; ^{31}P chemical shifts were referenced using external 85% H_3PO_4. Electrospray mass spectra were obtained with a Varian 500 MS LC Ion Trap Mass Spectrometer equipped with an

electrospray (ESI) ion source. For electrospray ionization, the drying gas and flow rate were optimized according to the particular sample with 35 p.s.i. nebulizer pressure. The compounds were observed in the positive mode (capillary voltage = 80–105 V). Gas chromatographic (GC) analyses were performed using a Fisons Instruments GC 8000 series gas chromatograph with DB-624 (J&W) capillary column (FID detector) and the Jasco-Borwin v.1.50 software. Catecholase activity studies were performed using an Agilent Cary 8454 UV-Visible Spectrophotometer with Agilent 89090A Peltier temperature controller and magnetic stirrer controller, and 845x UV-Vis System.

Synthesis of $[Cu^{II}(\mu\text{-}CH_3COO)_2(\kappa O\text{-}DAPTA{=}O)]_2$ (1). A round bottom flask fitted with a magnetic stirrer was charged with copper(II) acetate monohydrate (0.14 g**,** 0.7 mmol) and DAPTA (0.17 g, 0.7 mmol) in 25 mL toluene and 10 mL ethanol. The obtained green solution was stirred at room temperature for 8 hours then allowed to stand at ambient temperature with the flask closed for 2 weeks to obtain cyan crystals of **1** suitable for X-ray measurements. Yield, 31% (0.092 g, based on Cu).

FTIR (KBr, selected bands, in cm^{-1}): ν(C-H) 2943, *ν*(P=O) 1153, ν(C=O) 1627. Elemental analysis: calcd (%) for $C_{26}H_{44}Cu_2N_6O_{14}P_2$: C 36.58, H 5.19, N 9.84; found: C 35.86, H 4.80, N 8.78. ^{1}H NMR (400 MHz, DMSO, *δ*): 5.38 (d, *J* = 12 Hz, 2H, NC*H*$_2$N), 4.97–5.07 (br m, 2H, NC*H*$_2$N and 2H, PC*H*$_2$N), 4.81 (d, *J* = 12 Hz, 2H, NC*H*$_2$N), 4.60–4.71 (br m, 2H, PC*H*$_2$N), 4.37 (m, 2H, PC*H*$_2$N), 3.90 (m, 2H, PC*H*$_2$N), 3.72-3.81 (br m, 2H, NC*H*$_2$N and 4H, PC*H*$_2$N), 2.09 (s, 12H, NC(O)C*H*$_3$), 1.93 (br s, 12H, CuC(O)C*H*$_3$). ^{31}P{^{1}H} NMR (400 MHz, DMSO, *δ*): 2.95. ESI-MS$^+$ in H_2O (*m/z* assignment, % intensity): 449 ($[Cu(DAPTA{=}O)(CH_3COO)_2 + Na]^+$, 100), 246 ($[DAPTA{=}O + H]^+$, 71), 367 ($[Cu(DAPTA{=}O)(CH_3COO)]^+$, 36), 445 ($[Cu(DAPTA{=}O)(CH_3COO)_2 + H_2O + H]^+$, 30), 513 ($[2\ DAPTA{=}O + Na]^+$, 23), 612 ($[Cu(DAPTA{=}O)_2(CH_3COO)]^+$, 39).

Experiment with ^{18}O-labeled water. The above procedure for complex **1** preparation was repeated using freshly dried solvents in inert N_2 atmosphere and additional 50 µl of $H_2{}^{18}O$. The obtained cyan powder was isolated by filtration, washed with diethyl ether and dried in vacuum.

ESI-MS$^+$ in H_2O (*m/z* assignment, % intensity): 248 ($[DAPTA{=}O^{18} + H]^+$, 24), 288 ($[(DAPTA{=}O^{18} + H_2O + Na]^+$, 100), 369 ($[Cu(DAPTA{=}O^{18})(CH_3COO)]^+$, 14), 469

([Cu(DAPTA=O^{18})($CH_3COO)_2$ + H_2O + Na]$^+$, 40), 517 ([2 DAPTA=O^{18} + Na]$^+$, 15), 616 ([Cu(DAPTA=O^{18})$_2$(CH_3COO)]$^+$, 9).

Synthesis of [Na(1κ*OO'*;2κ*O*-DAPTA=O)(MeOH)]$_2$(BPh_4)$_2$ (2). A round bottom flask fitted with a magnetic stirrer was charged with DAPTA (0.23 g, 1 mmol), sodium tetraphenylborate Na(BPh_4) (0.34 g, 1 mmol) and nickel acetate hexahydrate Ni($CH_3COO)_2.6H_2O$ (0.29 g, 1 mmol) in 10 mL methanol. The obtained solution was stirred overnight at room temperature, then by slow diffusion of diethyl ether vapor at 4 °C, white crystals of **2** suitable for X-ray measurements were obtained. Yield, 32% (0.2 g, based on Na).

FTIR (KBr, selected bands, ν in cm^{-1}): ν(P=O) 1163, ν(C=O) 1631. Elemental analysis calcd (%) for $C_{68}H_{80}B_2N_6Na_2O_8P_2$: C 65.92, H 6.51, N 6.78; found: C 64.78, H 5.62, N 6.61. ^{1}H NMR (400 MHz, DMSO, *δ*): 7.71 (m, 16H, ArH Ph-C2,6-*H*), 6.92 (dd, $J_1 = J_2$ = 8 Hz, 16 H, ArH Ph-C3,5-*H*), 6.78 (dd, $J_1 = J_2$ = 8 Hz, 8 H, ArH Ph-C4-*H*), 5.59 (br s, 2H, *H*OCH_3), 5.39 (d, *J* = 12 Hz, 2H, NCH_2N), 4.97–5.08 (br m, 2H, NCH_2N and 2H, PCH_2N), 4.81 (d, *J* = 12 Hz, 2H, NCH_2N), 4.43 (m, 2H, PCH_2N), 4.37 (d, *J* = 16 Hz, 2H, PCH_2N), 4.02 (m, 2H, PCH_2N), 3.90 (d, *J* = 16 Hz, 2H, NCH_2N), 3.78 (d, *J* = 8 Hz, 4H, PCH_2N), 3.16 (s, 6 H, HOCH_3), 2.11 (s, 12H, C(O)CH_3). ^{31}P{^{1}H} NMR (400 MHz, DMSO, *δ*): 3.10. ESI-MS$^-$ in MeOH (*m/z* assignment, % intensity): 319 ([$(C_6H_5)_4B]^-$, 100). ESI-MS$^+$ in MeOH (*m/z* assignment, % intensity): 365 ([$(C_6H_5)_4B$ + 2Na]$^+$, 100), 300 ([Na(DAPTA=O)(MeOH)]$^+$, 13).

X-ray structure determinations. X-ray quality crystals of **1** and **2** were immersed in cryo-oil, mounted in a Nylon loop and measured at ambient temperature. Intensity data were collected using a Bruker AXS-KAPPA APEX II PHOTON 100 diffractometer with graphite monochromated Mo-Kα (0.71069 Å) radiation. Data were collected using omega scans of 0.5° per frame and full sphere of data were obtained. Cell parameters were retrieved using Bruker SMART[81] software and refined using Bruker SAINT[81] on all the observed reflections. Absorption corrections were applied using the SADABS program.[82] The structures were solved by direct methods using SIR97 package[83] and refined with SHELXL-2014/7.[84] Calculations were performed using the WinGX System-Version 2014.1.[85] The hydrogen atoms were included in the refinement using the riding-model approximation; U_{iso}(H) were defined as 1.2U_{eq} of the parent carbon atoms for phenyl and methylene residues,

and $1.5U_{eq}$ of the parent carbon atoms for methyl. The *O*-bound H-atom of the coordinated methanol was found in the difference Fourier map, the isotropic thermal parameter was set at 1.5 times the average thermal parameter of the oxygen atom and the position restrained by using the DFIX and DANG commands. Least square refinements with anisotropic thermal motion parameters for all the non-hydrogen atoms were employed. Crystallographic data and selected structural details for compounds **1** and **2** are listed in table 6.

Table 6. Crystal data and structure refinement details for complexes **1** and **2**.

	1	**2**
Empirical formula	$C_{26}H_{44}Cu_2N_6O_{14}P_2$	$C_{68}H_{80}B_2N_6Na_2O_8P_2$
Formula Weight	853.69	1238.92
Crystal system	triclinic	triclinic
Space group	*P* –1	P -1
Temperature/K	296 (2)	293(2)
a/Å	8.5049(12)	10.968(8)
b/Å	10.0708(13)	11.624(9)
c/Å	11.0145(15)	13.403(9)
α/°	96.825(5)	88.81(3)
β/°	98.513(5)	71.89(3)
γ/°	108.285(4)	77.02(3)
V (Å^3)	872.1(2)	1581(2)
Z	1	1
D_{calc} (g cm^{-3})	1.626	1.302
*F*000	442	656
μ(Mo Kα) (mm^{-1})	1.385	0.144
Rfls. collected/unique/observed	14577/ 3176/ 2191	22296/ 5842/ 3646
R_{int}	0.0934	0.0687
Final *R*1 [a], *wR*2 [b] ($I \geq 2\sigma$)	0.0433, 0.0779	0.0536, 0.1196
Goodness-of-fit on F^2	0.983	0.955

[a] $R = \Sigma||F_o|-|F_c||/\Sigma|F_o|$; [b] $wR(F^2) = [\Sigma w(|F_o|^2 - |F_c|^2)^2/\Sigma w|F_o|^4]^{½}$

Catalytic activity studies

Nitroaldol (Henry) reaction. In a typical experiment, the nitroalkane (1.5 mmol) was added to a solution of complex **1** (0.025 mmol) in 2 mL water, and the mixture was stirred for 15 minutes. The aldehyde (0.5 mmol) was added and the solution stirred in air under conditions and time intervals indicated in tables 2, 3 and 4. Then the mixture was diluted with 3 mL water and extracted three times with 10 mL of diethyl ether. The combined extracts were dried over anhydrous Na_2SO_4, and the mixture was then filtered off. After removal of diethyl ether under vacuum, the residue was taken for analysis by ^{1}H NMR spectroscopy, in $CDCl_3$,

in order to calculate the yield of obtained β-nitroalcohol, as no other products were detected (figures S2-4). The usage of ^{1}H NMR spectroscopy for the calculation of the obtained yields of β-nitroalcohols has proved to be effective in several other cases.[36,38,40,68,86–88] A number of ^{1}H NMR analyses were also performed in the presence of an internal standard (1,2-dimethoxyethane) to verify the efficiency of the procedure, giving yields similar to those obtained by the above method. The ratio between the *anti* and *syn* diastereoisomers of 1-phenyl-2-nitropropanol, obtained in the nitroaldol catalytic reaction using nitroethane, was also determined by ^{1}H NMR spectroscopy, as the values of vicinal coupling constants between the α-O–C–*H* and the α-N–C–*H* protons identify the isomers (J = 7–9 Hz for the *anti*-isomer, and J = 3.2–4 for the *syn*-isomer).[89,90]

Aerobic benzyl alcohol oxidation in aqueous medium. In a typical experiment, to a round bottom flask equipped with a condenser and a magnetic stirrer, benzyl alcohol (0.5 mmol) was added to 2 mL of 0.1 M K_2CO_3 aqueous solution, followed by catalyst **1** (0.025 mmol) and 2,2,6,6-tetramethylpiperidine-1-oxyl (TEMPO, 0.025 mmol). The obtained mixture was vigorously stirred under conditions and time intervals indicated in table 5 and in air. Eventually, the reaction mixture was neutralized with an appropriate amount of 1 M HCl and extracted with ethyl acetate. The organic phase was then analyzed by gas chromatography using cyclopentanone as internal standard.

Catecholase activity. The experiments were performed under aerobic conditions at constant stirring and temperature of 25ºC (monitored with a contact thermometer dipped in the solution). Measurements were performed using 1 cm path length quartz cuvette. In a typical test, the 6.73×10^{-5} – 1.35×10^{-2} M fresh methanol solutions of 3,5-di-*tert*-butylcatechol (3,5-dtbc) were treated with a 6.57×10^{-5} M methanol solution of compound **1** (1 – 205 equivalents). The absorbance was also measured at 390 nm (ε = 1518 $M^{-1}cm^{-1}$) as a function of time, over the first 5 min immediately after the addition of catalyst. Control experiment carried out under the same conditions but in the absence of copper(II) catalyst showed no conversion of 3,5-dtbc to 3,5-dtbq.

Computational Details

The full geometry optimization of all structures and transition states was carried out at the DFT level of theory using the M06 functional[91] with the help of the Gaussian-09 program package.[92] No symmetry operations were applied for any of the structures calculated. The geometry optimization was carried out using a relativistic Stuttgart pseudopotential which describes 10 core electrons and the appropriate contracted basis set (8s7p6d)/[6s5p3d] for the copper atom[93] and the 6-31G* basis set for other atoms. Single-point calculations were then performed on the basis of the equilibrium geometries found by using the 6-311+G** basis set for nonmetal atoms. The Hessian matrix was calculated analytically for all optimized structures to prove the location of correct minima (no imaginary frequencies) or saddle points (only one imaginary frequency) and to estimate the thermodynamic parameters, the latter being calculated at 25 °C. The nature of transition states was investigated by analysis of the vectors associated with the imaginary frequency and by calculations of the intrinsic reaction coordinates (IRC) by using the method developed by Gonzalez and Schlegel.[94–96]

The total energies corrected for solvent effects (E_s) were estimated at the single-point calculations on the basis of gas-phase geometries at the CPCM-M06/6-311+G**//gas-M06/6-31G* level of theory using the polarizable continuum model in the CPCM version[97,98] with methanol as the solvent. The dispersion, repulsion and cavitation terms were considered. The entropic term in solutions (S_s) was calculated according to the procedure described by Wertz[99] and Cooper and Ziegler[100] using equations (1)–(4):

$$\Delta S_1 = R\ln V^s_{m,liq}/V_{m,gas} \quad (1)$$

$$\Delta S_2 = R\ln V^\circ_m/V^s_{m,liq} \quad (2)$$

$$\alpha = \frac{S^{\circ,s}_{liq} - (S^{\circ,s}_{gas} + R\ln V^s_{m,liq}/V_{m,gas})}{(S^{\circ,s}_{gas} + R\ln V^s_{m,liq}/V_{m,gas})} \quad (3)$$

$$S_s = S_g + \Delta S_{sol} = S_g + [\Delta S_1 + \alpha(S_g + \Delta S_1) + \Delta S_2] =$$
$$S_g - 12.72 \text{ cal/mol•K} - 0.32(S_g - 12.72 \text{ cal/mol•K}) + 6.37 \text{ cal/mol•K} \quad (4)$$

where S_g is the gas-phase entropy of the solute, ΔS_{sol} is the solvation entropy, $S^{\circ,s}{}_{liq}$, $S^{\circ,s}{}_{gas}$ and $V^s{}_{m,liq}$ are the standard entropies and molar volumes of the solvent in the liquid or gas phases (127.2 and 239.9 J/mol•K and 40.46 mL/mol, respectively, for CH_3OH), $V_{m,gas}$ is the molar volume of the ideal gas at 25 °C (24450 mL/mol), $V^\circ{}_m$ is the molar volume of the solution that corresponds to the standard conditions (1000 mL/mol). The enthalpies and

Gibbs free energies in solution (H_s and G_s, respectively) were estimated using expressions (5) and (6)

$$H_s = E_s(6\text{-}311+G^{**}) + H_g(6\text{-}31G^{*}) - E_g(6\text{-}311+G^{**}) \quad (5)$$

$$G_s = H_s - TS_s \quad (6)$$

where E_s and E_g are the total energies in solution and the gas phase and H_g is the gas-phase enthalpy calculated at the corresponding level.

Supporting information

CCDC 1576097 (for **1**) and 1576098 (for **2**) contain the supplementary crystallographic data for this paper. This data can be obtained free of charge from The Cambridge Crystallographic Data Center via www.ccdc.cam.ac.uk/data_request/cif.

Acknowledgements

This work has been partially supported by the Foundation for Science and Technology (FCT), (UID/QUI/00100/2013), Portugal and NCN program (Grant No. 2012/07/B/ST/00885), Poland. A. G. M. is thankful to the CATSUS doctoral program of FCT for his PhD fellowship (SFRH/BD/106006/2014). The authors acknowledge the Portuguese NMR Network (IST-UL Center) for access to the NMR facility and the IST Node of the Portuguese Network of Mass-spectrometry for the ESI-MS measurements. Piotr Jakimowicz (Faculty of Biotechnology, University of Wroclaw, Wroclaw, Poland) was acknowledged for his assistance in the catechol oxidation studies.

References:

[1] A. D. Phillips, L. Gonsalvi, A. Romerosa, F. Vizza, M. Peruzzini, *Coord. Chem. Rev.* **2004**, *248*, 955–993.

[2] J. Bravo, S. Bolaño, L. Gonsalvi, M. Peruzzini, *Coord. Chem. Rev.* **2010**, *254*, 555–607.

[3] A. Guerriero, M. Peruzzini, L. Gonsalvi, *Coord. Chem. Rev.* **2018**, *355*, 328–361.

[4] X. Tu, G. S. Nichol, Z. Zheng, *J. Clust. Sci.* **2009**, *20*, 93–103.

[5] A. M. Kirillov, M. Filipowicz, M. F. C. Guedes da Silva, J. Kłak, P. Smoleński, A. J. L. Pombeiro, *Organometallics* **2012**, *31*, 7921–7925.

[6] P. Smoleński, J. Kłak, D. S. Nesterov, A. M. Kirillov, *Cryst. Growth Des.* **2012**, *12*, 5852–5857.

[7] A. M. Kirillov, P. Smoleński, M. F. C. Guedes da Silva, A. J. L. Pombeiro, *Eur. J. Inorg. Chem.* **2007**, 2686–2692.

[8] A. M. Kirillov, P. Smoleński, M. F. C. Guedes da Silva, M. N. Kopylovich, A. J. L. Pombeiro, *Acta Crystallogr. Sect. E Struct. Reports Online* **2008**, *64*, m603–m604.

[9] A. M. Kirillov, P. Smoleński, M. Haukka, M. F. C. Guedes da Silva, A. J. L. Pombeiro, *Organometallics* **2009**, *28*, 1683–1687.

[10] A. M. Kirillov, P. Smoleński, Z. Ma, M. F. C. Guedes Da Silva, M. Haukka, A. J. L. Pombeiro, *Organometallics* **2009**, *28*, 6425–6431.

[11] (a) V. I. Siele, J. Heterocycl. Chem., 1977, 14, 337–339. b) A. Mena-Cruz, P. Lorenzo-Luis, A. Romerosa, M. Saoud, M. Serrano-Ruiz, *Inorg. Chem.* **2007**, *46*, 6120–6128; (c) A. Mena-Cruz, P. Lorenzo-Luis, A. Romerosa, M. Serrano-Ruiz, *Inorg. Chem.* **2008**, *47*, 2246–2248.; (d) A. Mena-Cruz, P. Lorenzo-Luis, V. Passarelli, A. Romerosa, M. Serrano-Ruiz, *Dalton Trans.* **2011**, *40*, 3237–3244; (e) M. Serrano-Ruiz, L. M. Aguilera-Sáez, P. Lorenzo-Luis, J. M. Padrón, A. Romerosa, *Dalton Trans.* **2013**, *42*, 11212–11219; (f) Z. Mendoza, P. Lorenzo-Luis, M. Serrano-Ruiz, E. Martín-Batista, J. M. Padrón, F. Scalambra, A. Romerosa, *Inorg. Chem.* **2016**, *55*, 7820–7822; (g) Z. Mendoza, P. Lorenzo-Luis, F. Scalambra, J. M. Padrón, A. Romerosa, *Dalton Trans.* **2017**, *46*, 8009–8012.

[12] V. I. Siele, *J. Heterocycl. Chem.* **1977**, *14*, 337–339.

[13] D. J. Darensbourg, C. G. Ortiz, J. W. Kamplain, *Organometallics* **2004**, *23*, 1747–1754.

[14] V. Gandin, A. Trenti, M. Porchia, F. Tisato, M. Giorgetti, I. Zanusso, L. Trevisi, C. Marzano, *Metallomics* **2015**, *7*, 1497–1507.

[15] P. Nowak-Sliwinska, J. R. van Beijnum, A. Casini, A. A. Nazarov, G. Wagnières, H. van den Bergh, P. J. Dyson, A. W. Griffioen, *J. Med. Chem.* **2011**, *54*, 3895–3902.

[16] E. Vergara, E. Cerrada, C. Clavel, A. Casini, M. Laguna, *Dalton Trans.* **2011**, *40*, 10927–10935.

[17] E. Guerrero, S. Miranda, S. Lüttenberg, N. Fröhlich, J.-M. Koenen, F. Mohr, E.

Cerrada, M. Laguna, A. Mendía, *Inorg. Chem.* **2013**, *52*, 6635–6647.

[18] J. García-Álvarez, J. Díez, J. Gimeno, F. J. Suárez, C. Vincent, *Eur. J. Inorg. Chem.* **2012**, 5854–5863.

[19] E. Bolyog-Nagy, A. Udvardy, F. Joó, Á. Kathó, *Tetrahedron Lett.* **2014**, *55*, 3615–3617.

[20] E. Tomás-Mendivil, R. García-Álvarez, C. Vidal, P. Crochet, V. Cadierno, *ACS Catal.* **2014**, *4*, 1901–1910.

[21] A. G. Mahmoud, M. F. C. Guedes da Silva, J. Sokolnicki, P. Smoleński, A. J. L. Pombeiro, *Dalton Trans.* **2018**, *47*, 7290–7299.

[22] E. Vergara, S. Miranda, F. Mohr, E. Cerrada, E. R. T. Tiekink, P. Romero, A. Mendía, M. Laguna, *Eur. J. Inorg. Chem.* **2007**, *2007*, 2926–2933.

[23] F. Mohr, S. Sanzb, E. Vergarab, E. Cerradab, M. Laguna, *Gold Bull.* **2006**, *39*, 212–215.

[24] J. Braddock-Wilking, S. Acharya, N. P. Rath, *Polyhedron* **2014**, *79*, 16–28.

[25] B. J. Frost, J. L. Harkreader, C. M. Bautista, *Inorg. Chem. Commun.* **2008**, *11*, 580–583.

[26] T. F. S. Silva, P. Smoleński, L. M. D. R. S. Martins, M. F. C. Guedes da Silva, A. R. Fernandes, D. Luis, A. Silva, S. Santos, P. M. Borralho, C. M. P. Rodrigues, et al., *Eur. J. Inorg. Chem.* **2013**, *2013*, 3651–3658.

[27] B. J. Frost, W.-C. Lee, K. Pal, T. H. Kim, D. VanDerveer, D. Rabinovich, *Polyhedron* **2010**, *29*, 2373–2380.

[28] A. M. Kirillov, S. W. Wieczorek, A. Lis, M. F. C. Guedes da Silva, M. Florek, J. Król, Z. Staroniewicz, P. Smoleński, A. J. L. Pombeiro, *Cryst. Growth Des.* **2011**, *11*, 2711–2716.

[29] M. Rancan, J. Tessarolo, M. Casarin, P. L. Zanonato, S. Quici, L. Armelao, *Inorg. Chem.* **2014**, *53*, 7276–7287.

[30] M. Rancan, J. Tessarolo, S. Quici, L. Armelao, *Chem. Commun.* **2014**, *50*, 13761–13764.

[31] G. Rosini, in *Compr. Org. Synth.* (Eds.: B.M. Trost, I. Fleming, C.H. Heathcock), **1991**, pp. 321–340.

[32] F. A. Luzzio, *Tetrahedron* **2001**, *57*, 915–945.

[33] E. W. Colvin, A. K. Beck, D. Seebach, *Helv. Chim. Acta* **1981**, *64*, 2264–2271.

[34] G. Rosini, R. Ballini, M. Petrini, E. Marotta, P. Righi, *Org. Prep. Proced. Int.* **1990**, *22*, 707–746.

[35] G. D. Buckley, C. W. Scaife, *J. Chem. Soc.* **1947**, 1471–1472.

[36] M. N. Kopylovich, T. C. O. Mac Leod, K. T. Mahmudov, M. F. C. Guedes da Silva, A. J. L. Pombeiro, *Dalton Trans.* **2011**, *40*, 5352–5361.

[37] M. Sutradhar, M. F. C. Guedes da Silva, A. J. L. Pombeiro, *Catal. Commun.* **2014**, *57*, 103–106.

[38] A. P. C. Ribeiro, Y. Y. Karabach, L. M. D. R. S. Martins, A. G. Mahmoud, M. F. C. Guedes da Silva, A. J. L. Pombeiro, *RSC Adv.* **2016**, *6*, 29159–29163.

[39] R. Ballini, G. Bosica, *J. Org. Chem.* **1997**, *62*, 425–427.

[40] C. Christensen, K. Juhl, R. G. Hazell, K. A. Jørgensen, *J. Org. Chem.* **2002**, *67*, 4875–4881.

[41] S.-F. Lu, D.-M. Du, S.-W. Zhang, J. Xu, *Tetrahedron: Asymmetry* **2004**, *15*, 3433–3441.

[42] M. V. N. De Souza, *Mini. Rev. Org. Chem.* **2006**, *3*, 155–165.

[43] T. Vogler, A. Studer, *Synthesis (Stuttg).* **2008**, *2008*, 1979–1993.

[44] S. Hazra, L. M. D. R. S. Martins, M. F. C. Guedes da Silva, A. J. L. Pombeiro, *RSC Adv.* **2015**, *5*, 90079–90088.

[45] M. Sutradhar, L. M. D. R. S. Martins, M. F. C. Guedes da Silva, A. J. L. Pombeiro, *Appl. Catal. A Gen.* **2015**, *493*, 50–57.

[46] A. Karmakar, L. M. D. R. S. Martins, M. F. C. Guedes da Silva, S. Hazra, A. J. L. Pombeiro, *Catal. Letters* **2015**, *145*, 2066–2076.

[47] K. T. Mahmudov, M. Sutradhar, L. M. D. R. S. Martins, M. F. C. Guedes da Silva, A. Ribera, A. V. M. Nunes, S. I. Gahramanova, F. Marchetti, A. J. L. Pombeiro, *RSC Adv.* **2015**, *5*, 25979–25987.

[48] I. A. Koval, P. Gamez, C. Belle, K. Selmeczi, J. Reedijk, *Chem. Soc. Rev.* **2006**, *35*, 814–840.

[49] M. Gupta, P. Mathur, R. J. Butcher, *Inorg. Chem.* **2001**, *40*, 878–885.

[50] M. Merkel, N. Möller, M. Piacenza, S. Grimme, A. Rompel, B. Krebs, *Chem. - A Eur. J.* **2005**, *11*, 1201–1209.

[51] K. Shanmuga Bharathi, S. Sreedaran, R. Anitha Ayswarya, A. Kalilur Rahiman, K. Rajesh, V. Narayanan, *J. Coord. Chem.* **2009**, *62*, 600–612.

[52] R. E. H. M. B. Osório, A. Neves, T. P. Camargo, S. L. Mireski, A. J. Bortoluzzi, E. E. Castellano, W. Haase, Z. Tomkowicz, *Inorganica Chim. Acta* **2015**, *435*, 153–158.

[53] J. Mukherjee, R. Mukherjee, *Inorganica Chim. Acta* **2002**, *337*, 429–438.

[54] L. M. Mirica, X. Ottenwaelder, T. D. P. Stack, *Chem. Rev.* **2004**, *104*, 1013–1046.

[55] P. C. A. Bruijnincx, G. van Koten, R. J. M. Klein Gebbink, *Chem. Soc. Rev.* **2008**, *37*, 2716–2744.

[56] Á. Kupán, J. Kaizer, G. Speier, M. Giorgi, M. Réglier, F. Pollreisz, *J. Inorg. Biochem.* **2009**, *103*, 389–395.

[57] S. Majumder, S. Sarkar, S. Sasmal, E. C. Sañudo, S. Mohanta, *Inorg. Chem.* **2011**, *50*, 7540–7554.

[58] S. Anbu, A. Paul, A. P. C. Ribeiro, M. F. C. Guedes da Silva, M. L. Kuznetsov, A. J. L. Pombeiro, *Inorganica Chim. Acta* **2016**, *450*, 426–436.

[59] V. K. Bhardwaj, N. Aliaga-Alcalde, M. Corbella, G. Hundal, *Inorganica Chim. Acta* **2010**, *363*, 97–106.

[60] S. K. Dey, A. Mukherjee, *Coord. Chem. Rev.* **2016**, *310*, 80–115.

[61] S. W. Jaros, P. Smolenski, M. F. C. Guedes da Silva, M. Florek, J. Król, Z. Staroniewicz, A. J. L. Pombeiro, A. M. Kirillov, *CrystEngComm* **2013**, *15*, 8060–8064.

[62] P. Smoleński, M. V. Kirillova, M. F. C. Guedes da Silva, A. J. L. Pombeiro, *Dalton Trans.* **2013**, *42*, 10867–10874.

[63] S. W. Jaros, M. F. C. Guedes da Silva, M. Florek, M. C. Oliveira, P. Smoleński, A. J. L. Pombeiro, A. M. Kirillov, *Cryst. Growth Des.* **2014**, *14*, 5408–5417.

[64] P. Smoleński, A. M. Kirillov, M. F. C. Guedes da Silva, A. J. L. Pombeiro, *Inorganica Chim. Acta* **2011**, *378*, 342–346.

[65] A. W. Addison, T. N. Rao, J. Reedijk, J. van Rijn, G. C. Verschoor, *J. Chem. Soc. Dalton Trans.* **1984**, 1349–1356.

[66] L. Yang, D. R. Powell, R. P. Houser, *Dalton Trans.* **2007**, 955–964.

[67] D. A. Evans, D. Seidel, M. Rueping, H. W. Lam, J. T. Shaw, C. W. Downey, *J. Am. Chem. Soc.* **2003**, *125*, 12692–12693.

[68] N. Q. Shixaliyev, A. M. Maharramov, A. V. Gurbanov, V. G. Nenajdenko, V. M. Muzalevskiy, K. T. Mahmudov, M. N. Kopylovich, *Catal. Today* **2013**, *217*, 76–79.

[69] A. Karmakar, M. F. C. Guedes da Silva, A. J. L. Pombeiro, *Dalton Trans.* **2014**, *43*,

7795–7810.

[70] A. Karmakar, S. Hazra, M. F. C. Guedes da Silva, A. J. L. Pombeiro, *New J. Chem.* **2014**, *38*, 4837–4846.

[71] A. Paul, A. Karmakar, M. F. C. Guedes da Silva, A. J. L. Pombeiro, *RSC Adv.* **2015**, *5*, 87400–87410.

[72] A. Karmakar, S. Hazra, M. F. C. Guedes da Silva, A. Paul, A. J. L. Pombeiro, *CrystEngComm* **2016**, *18*, 1337–1349.

[73] A. Karmakar, L. M. D. R. S. Martins, S. Hazra, M. F. C. Guedes da Silva, A. J. L. Pombeiro, *Cryst. Growth Des.* **2016**, *16*, 1837–1849.

[74] P. Gamez, I. W. C. E. Arends, R. A. Sheldon, J. Reedijk, *Adv. Synth. Catal.* **2004**, *346*, 805–811.

[75] P. J. Figiel, M. Leskelä, T. Repo, *Adv. Synth. Catal.* **2007**, *349*, 1173–1179.

[76] R. Marion, M. Zaarour, N. A. Qachachi, N. M. Saleh, F. Justaud, D. Floner, O. Lavastre, F. Geneste, *J. Inorg. Biochem.* **2011**, *105*, 1391–1397.

[77] K. Selmeczi, M. Réglier, M. Giorgi, G. Speier, *Coord. Chem. Rev.* **2003**, *245*, 191–201.

[78] R. Sanyal, S. Ketkov, S. Purkait, F. A. Mautner, G. Zhigulin, D. Das, *New J. Chem.* **2017**, *41*, 8586–8597.

[79] K. S. Banu, T. Chattopadhyay, A. Banerjee, S. Bhattacharya, E. Suresh, M. Nethaji, E. Zangrando, D. Das, *Inorg. Chem.* **2008**, *47*, 7083–7093.

[80] M. Louloudi, K. Mitopoulou, E. Evaggelou, Y. Deligiannakis, N. Hadjiliadis, *J. Mol. Catal. A Chem.* **2003**, *198*, 231–240.

[81] *Bruker, APEX2. Bruker AXS Inc., Madison, Wisconsin, USA,* **2012**.

[82] *G.M. Sheldrick, SADABS. Program for Empirical Absorption Correction. University of Gottingen, Germany,* **2000**.

[83] A. Altomare, M. C. Burla, M. Camalli, G. L. Cascarano, C. Giacovazzo, A. Guagliardi, A. G. G. Moliterni, G. Polidori, R. Spagna, *J. Appl. Crystallogr.* **1999**, *32*, 115–119.

[84] G. M. Sheldrick, IUCr, *Acta Crystallogr. Sect. A Found. Crystallogr.* **2008**, *64*, 112–122.

[85] L. J. Farrugia, *J. Appl. Crystallogr.* **2012**, *45*, 849–854.

[86] A. Cwik, A. Fuchs, Z. Hell, J.-M. Clacens, *Tetrahedron* **2005**, *61*, 4015–4021.

[87] K. R. Reddy, C. V. Rajasekhar, G. G. Krishna, *Synth. Commun.* **2007**, *37*, 1971–1976.

[88] S. Jammi, M. A. Ali, S. Sakthivel, L. Rout, T. Punniyamurthy, *Chem. - An Asian J.* **2009**, *4*, 314–320.

[89] S. E. Denmark, B. S. Kesler, Y. C. Moon, *J. Org. Chem.* **1992**, *57*, 4912–4924.

[90] V. J. Bulbule, V. H. Deshpande, S. Velu, A. Sudalai, S. Sivasankar, V. T. Sathe, *Tetrahedron* **1999**, *55*, 9325–9332.

[91] Y. Zhao, D. G. Truhlar, *Theor. Chem. Acc.* **2008**, *120*, 215–241.

[92] M. J. Frisch, G. W. Trucks, H. B. Schlegel, G. E. Scuseria, M. A. Robb, J. R. Cheeseman, G. Scalmani, V. Barone, B. Mennucci, G. A. Petersson, H. Nakatsuji, M. Caricato, X. Li, H. P. Hratchian, A. F. Izmaylov, J. Bloino, G. Zheng, J. L. Sonnenberg, M. Hada, M. Ehara, K. Toyota, R. Fukuda, J. Hasegawa, M. Ishida, T. Nakajima, Y. Honda, O. Kitao, H. Nakai, T. Vreven, J. A. J. Montgomery, J. E. Peralta, F. Ogliaro, M. Bearpark, J. J. Heyd, E. Brothers, K. N. Kudin, V. N. Staroverov, R. Kobayashi, J. Normand, K. Raghavachari, A. Rendell, J. C. Burant, S. S. Iyengar, J. Tomasi, M. Cossi, N. Rega, J. M. Millam, M. Klene, J. E. Knox, J. B. Cross, V. Bakken, C. Adamo, J. Jaramillo, R. Gomperts, R. E. Stratmann, O. Yazyev, A. J. Austin, R. Cammi, C. Pomelli, J. W. Ochterski, R. L. Martin, K. Morokuma, V. G. Zakrzewski, G. A. Voth, P. Salvador, J. J. Dannenberg, S. Dapprich, A. D. Daniels, O. Farkas, J. B. Foresman, J. V. Ortiz, J. Cioslowski, D. J. Fox, *Gaussian 09, Revis. A.01; Gaussian, Inc., Wallingford, CT* **2009**.

[93] M. Dolg, U. Wedig, H. Stoll, H. Preuss, *J. Chem. Phys.* **1987**, *86*, 866–872.

[94] C. Gonzalez, H. B. Schlegel, *J. Chem. Phys.* **1989**, *90*, 2154–2161.

[95] C. Gonzalez, H. B. Schlegel, *J. Phys. Chem.* **1990**, *94*, 5523–5527.

[96] C. Gonzalez, H. B. Schlegel, *J. Chem. Phys.* **1991**, *95*, 5853–5860.

[97] J. Tomasi, M. Persico, *Chem. Rev.* **1994**, *94*, 2027–2094.

[98] V. Barone, M. Cossi, *J. Phys. Chem. A* **1998**, *102*, 1995–2001.

[99] D. H. Wertz, *J. Am. Chem. Soc.* **1980**, *102*, 5316–5322.

[100] J. Cooper, T. Ziegler, *Inorg. Chem.* **2002**, *41*, 6614–6622.